

Synthesis, characterization and hydration analysis of a novel epoxy/superplasticizer oilwell cement slurry – Some mechanistic features by solution microcalorimetry

Antonio R. Cestari^{*}, Eunice F.S. Vieira, Ellen C.S. Silva, Fernanda J. Alves, Marcos A.S. Andrade Jr.

Laboratory of Materials and Calorimetry, Department of Chemistry/CCET, Federal University of Sergipe, 49100-000 São Cristóvão, Sergipe, Brazil

ARTICLE INFO

Article history:

Received 26 January 2012

Accepted 16 April 2012

Available online 27 April 2012

Keywords:

Oilwell cement slurries

Epoxy resins

Polyacrylates

Solution microcalorimetry

Eco-friendly materials

Superplasticizers

Solution calorimetry

Kinetic modeling

ABSTRACT

A new epoxy/polyacrylate-modified oilwell cement slurry was synthesized. The features of the new slurry were evaluated in relation to a standard cement slurry ($w/c = 0.5$). The characterization of the slurries was performed by Raman, XRD, TG/DTG and solid-state diffuse reflectance spectroscopy. The main morphological features of the new slurry were preserved, even after long-term contact with HCl in aqueous solution. The hydration of the slurries was studied by heat-conduction microcalorimetry. The exothermic microcalorimetric outputs were well fitted to a three-parameter kinetic model. The analysis of both thermodynamic and kinetic results from microcalorimetry have pointed out that diffusional growth from non-stoichiometric mixtures is the main mechanistic feature of the hydration of the cement slurries. The results of this study underline the excellent features of the new epoxy/superplasticizer-modified cement slurry for using in severe acidic environments of oilwells.

© 2012 Elsevier Inc. All rights reserved.

1. Introduction

Oilwell cementing is used for providing zonal isolation of subterranean formations to prevent exchange of gas or fluids among different geological formations, as well as for protecting oil producing zones from collapse. Oilwell cementing is less tolerant to errors than conventional cementing works [1,2]. If the cement does not provide a good seal, gas or liquid fluids can migrate to the surface and lead to work accidents or environmental problems [1]. So, fully understanding of interfacial phenomena behind oilwell cement procedures has scientific, economic and environmental importance.

In order to increase the production of oilwells, one such method commonly employed in oil and gas industry is known as acidizing stimulation [3]. Typically, a non-oxidizing mineral acid is introduced into the well and is forced into subterranean formations to remove acid-reactive components, such as carbonates of alkali metals and others. The usual acid employed in such acidizing procedures is hydrochloric acid. However, several oilwells have been observed to exhibit well zonal intercommunication problems due to problems in the cement slurries. It is due to reactions between the hardened slurries in the oilwell annulus and the acidic solution. As a consequence, acid (even oil) spill may cause long-term environmental problems [3,4]. In this way, cementing of oilwells requires new materials that provide long-term stability in acidic

media. The protective characteristics of oilwell cements may be controlled by the addition of polymeric additives [5].

The use of specific polymeric nets has been highly effective in preventing destruction and increasing the internal cohesion of oilwell cement packs. In this way, epoxy resins are useful to promote physico-chemical interactions and ensure excellent levels of adhesion between the mineral and organic phases of polymer-modified cement slurries [5,6]. In this way, polymeric nets of epoxy resins are typically insoluble in the aqueous mineral acid solutions employed in acidizing operations of oilwells. Epoxy cements are composed of epoxy resin, cement and fine aggregates. Epoxy resin systems are made up of an epoxy resin and a curing agent (also called a hardener or catalyst). Common epoxy formulations are based on diglycidyl ether of bisphenol A resins that can be cross-linked with a wide variety of hardeners such as amines, organic acids, anhydrides and others [7].

It is well known that hydration phenomena at cement and water interfaces drive the characteristics of oilwell cement slurries. The knowledge of the heat-producing properties during oilwell cement hydration is required to choose a suitable cementitious system for a given specific project. The kinetic and thermodynamic features of the early hydration stages are essential for the performance of hardened cements and can be monitored by microcalorimetry [8,9]. Heat-conduction microcalorimetry has been used to obtain and analyze the features of heat evolution evolved in the early stages of hydration of cement slurries, with the objective of increasing understanding of the hydration mechanisms at cement

^{*} Corresponding author. Fax: +55 79 21056684.

E-mail address: cestari@ufs.br (A.R. Cestari).

and water interfaces. However, there is relatively little research on early cement hydration, that is, the initial hours after adding water.

In this work, it is intended to use sodium polyacrylate as a superplasticizer agent in a new epoxy-cement system for use in routine oilwell operations. Superplasticizers can be used for three different purpose, namely (a) to increase workability without changing the mixture composition, (b) to reduce the amount of mixing water in order to reduce the water-to-cement ratio and then to increase strength and/or improve durability, and (c) to reduce both water and cement in order to reduce cost in addition to reducing creep, shrinkage and thermal strains caused by heat of cement hydration [10]. As far as we known, nothing is known about the role of the epoxy/superplasticizer system in oilwell cement procedures. The features of the new slurry were evaluated in relation to a standard cement slurry ($w/c = 0.5$). The structural characterization of the slurries, before and after contact with aqueous HCl solution, is also presented and discussed.

2. Experimental section

2.1. Materials and reagents

Water was used after double distillation. Powder cement (200–325 mesh, Class A special for oilwell cementation) from Cimesa Special Cements (Laranjeiras, Brazil) and silica gel of 150–300 mesh (particles diameter) from Schumberger Petroleum Services (Nossa Senhora do Socorro/SE, Brazil) were used in the slurries preparations. The bisphenol A epoxy resin, commercially available as Araldite GY279, as well as its hardener (Aradur 2963), was supplied by The Huntsman Co Special Resins. Sodium polyacrylate was obtained from Sigma–Aldrich. The idealized chemical structures of the epoxy resin, the hardener and sodium polyacrylate are shown in Fig. 1.

2.2. Preparation of the cement slurries

The mixing procedure adopted in accordance with the American Petroleum Institute (API) practice was described earlier [8,9]. It was consisted of mixing the cement, epoxy resin and hardener, sodium polyacrylate and water for 30 s at 12,000 rpm. The amounts

of the components of the slurries were calculated in relation to a final density of the cured slurries from 1.50 to 2.00 g cm⁻³ [8,9].

In order to avoid uncompleted polymerization, the proportion of epoxy resin/hardener was 1:2. The cement, silica and water were used to obtain the standard cement slurry ($w/c = 0.5$) for comparative purposes. The cement slurries were cast into cubic molds with 5.08 cm sides and cured in water for 28 days before use. For simplicity, the slurries are hereafter denominated as epoxy-sp (cement, water, silica, epoxy resin, hardener and superplasticizer) and standard (cement, silica and water).

2.3. Characterization of the cement slurries

The Raman spectra were acquired with a Bruker Senterra Raman System equipped with an Olympus microscope with a 50× objective to focus a Melles Griot laser beam on the sample. The spectra were excited by the 785 nm line from an air-cooled He–Ne laser. The laser power measured after the microscope objective was ca. 50 mW. The thermogravimetric analyses (TG and DTG) were made using about 10 mg of material, under synthetic air atmosphere from 25 to 800 °C, in a SDT 2960 thermoanalyzer, from TA Instruments. DRX-ray analyses were performed in a Shimadzu diffractometer, in the 2θ range from 5° to 60° (accumulation rate of 0.02° min⁻¹), using Cu K α radiation. The solid-state diffuse reflectance spectra of the samples were recorded on an Ocean Optics UV–Vis spectrophotometer from 400 to 900 cm⁻¹ at a resolution of 4.0 cm⁻¹.

The cement samples were also characterized after 40 h in contact with a 0.1 mol L⁻¹ aqueous solution of HCl. From earlier studies [8,9], this contact time is sufficient to reach the maximum HCl amounts sorbed on oilwell cement slurries.

3. Results and discussion

3.1. Some considerations on cement chemistry, epoxy resins and superplasticizers

Cured cements have a range of sizes and complex internal microstructures, with the result that different clinker phases hydrate at different rates. The composition of oilwell cement slurries is usually based upon four principal mineral phases [1]: tricalcium silicate (Ca₃SiO₅, or C₃S), dicalcium silicate (Ca₂SiO₄, or C₂S), tricalcium aluminate (Ca₃Al₂O₆, or C₃A), and a calcium aluminoferrite (C₄AF) of variable composition. These mineral phases are intimately mixed in the form of cement grains, with little or no pore space.

At ambient temperature, the most important cement hydration process is the conversion of the silicate phases to an almost amorphous C–S–H and portlandite (Ca(OH)₂). The calcium silicate hydrate (C–S–H) formed is typically a poorly crystalline non-stoichiometric material consisting principally of dimeric units at first, but which subsequently slowly polymerizes after a few days. The portlandite released during cement hydration is partially consumed as a result of interaction with active silica fume to form C–S–H phases. In general, sulfate is added to all cements in the form of calcium sulfate. If not, the C₃A and C₄AF phases may quickly hydrate and cause loss of workability [11].

The most rapid reaction during the early hours of cement hydration at ambient temperature is due to the formation of ettringite, a hydrous calcium aluminumsulfate mineral (Ca₆Al₂(SO₄)₃(OH)₁₂·26H₂O). The C₂S phases react at a much slower rate to form similar hydration products. Some portlandite is present at the beginning of hydration, where the aqueous phase of the cement slurry can be considered for simplicity as essentially a

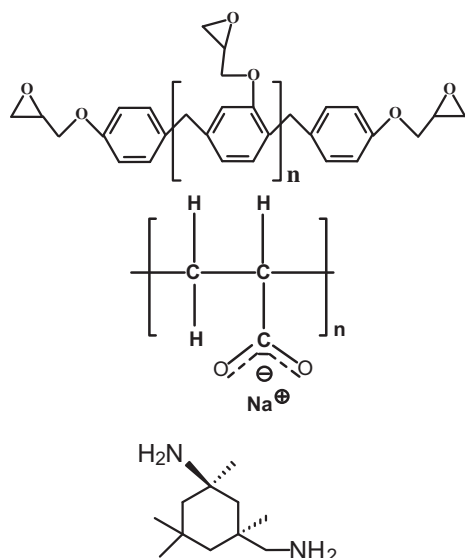


Fig. 1. Idealized chemical structures of the epoxy resin (above) and sodium polyacrylate (center) and the hardener (below).

limewater medium, being derived from some hydration of the CaO content as follows [12]:



One of the most common additives in cement admixture both in oil field industry is silica flour, which is typically a highly effective pozzolanic material in nature [13]. In oilwell cement industry, silica is a lightener agent due to the fineness of the particles and is added to prevent strength degradation by forming crystalline calcium silicate hydrates. Literature data have demonstrated that tiny particles of silica reduce the setting time, porosity and permeability and increase the strength (compressive, tensile) of cement slurries [12,13].

The presence of water-soluble polymers in cement mortars influences the rate and degree of cement hydration and the nature and amount of hydration products that are formed. Additionally, the morphology of the hydrate crystals and the microstructure of the cement paste are changed. This is due to partial intercalation of the polymer chains within the cement hydrate lattice [14]. During hardening, two processes can take place, that is, cement hydration and polymer film formation. In general, organic polymeric additives have shown to strongly interact with the surface of hydrated C–S–H, controlling the pathways or mechanism of the interaction between the organic molecules [15].

Cement mortars modified with water-soluble polymers show higher water retention than ordinary cement mortars. The hydrophilic parts of the polymers interact with the water molecules in the fresh mixture, preventing the dry-out by evaporation and absorption into the surrounding porous material [1]. The water retaining capacity also often results in a thickening and viscosity enhancing behavior. Because of the increased viscosity of the cement paste, less free water is available for bleeding and the segregation tendency decreases. So, the homogeneity of the mortar is improved.

The epoxy-amine system cure progressively transforms an initially fluid small-molecule mixture into an insoluble network [7]. However, the chemistry involved in the epoxy/amine curing process is rather complex and still not completely understood. An idealized structure of polymerized amine-crosslinked epoxy resins is shown in Fig. 2. In general, there are several reactions participating in the epoxy/amine-hardener network formation.

Competitive chemical reactions accompanied by complex physical phenomena occur during curing, when the system passes from

a mixture of linear and branched oligo- and polymers into a single, three-dimensional, macromolecule [16]. For an epoxy cure with primary amine groups of an amine-hardener, at least four reactions can occur. The first reaction is between an epoxide ring and a primary amine to produce a secondary amine and a hydroxyl group (–OH). The formed secondary amine can also react with an epoxide to produce a tertiary amine and a new –OH group. Another possible reaction is the etherification between a –OH group of a secondary amine and an epoxide to form an ether link and a new –OH group. In general, the primary amine sites in this system act as chain extenders while the secondary amines produce branched and crosslinked structures [16].

Superplasticizers, also known as high-range water-reducing admixtures, are highly efficient water reducers. Anionic long-chain molecules of the admixture become adsorbed on the surface of the cement particles that are effectively dispersed in water through electrical repulsion. The alkaline solution resulting from the hydration of Portland cement gradually hydrolyzes the superplasticizer, releasing a water-soluble dispersant that helps to maintain the initial slump for a long time. The crosslinked polymer is hydrolyzed by the alkaline water phase of the cement paste and then converted into an acrylic polymer. Practical examples of these different ways of using superplasticizers are given by referring to the recent advances in this area using polyacrylate-based admixtures [17].

Superplasticizers cause dispersion into smaller agglomerates of cement particles which predominate in the cement paste of the concrete mixture. Due to the dispersion effect, there is a fluidity increase in the cement mixture. The attractive forces existing among cement particles and causing polymers negatively charged, such as polyacrylates, for the presence of anionic groups on the surface of cement particles. The dispersion of cement particles would be related with the electrical repulsion produced by the adsorption of negatively charged groups on cement particles. It would seem that the polymer adsorption itself rather than the electrostatic repulsion is responsible for the dispersion of large agglomerates of cement particles into smaller ones resulting in a remarkable increase in the fluidity of cement mixtures.

Both the steric hindrance effect and the electrical repulsive force due to the negative carboxylic groups would be responsible for the dispersion of cement particles and the fluidizing action of the admixture. The dispersion mechanism performed by superplasticizers could be related to a steric hindrance effect (produced

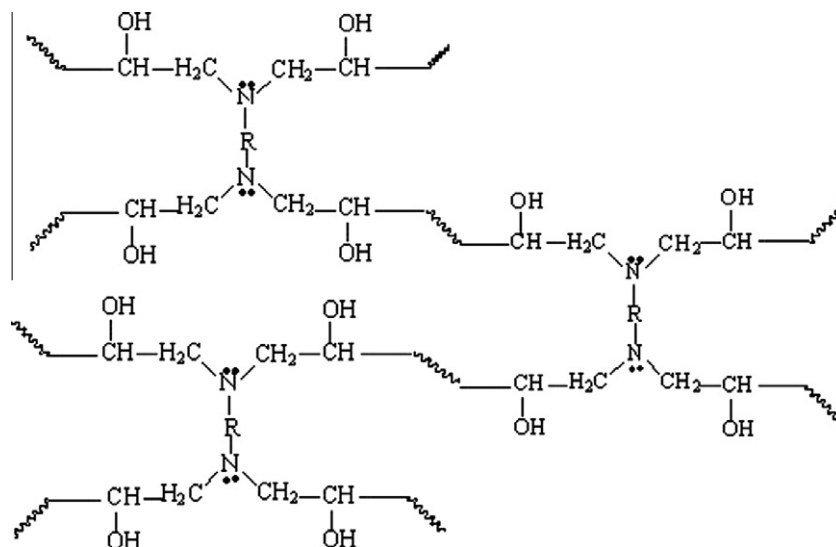


Fig. 2. Idealized structure of polymerized amine-crosslinked epoxy resins.

by the presence of side long graft chains) rather than to the presence of negatively charged anionic groups (typically COO^-) [18]. In other words, the graft chains of the polymer molecules on the surface of cement would hinder by themselves from flocculating into large and irregular agglomerates of cement particles. The fluidizing effect of superplasticizer is also influenced by the type of cement used. In general, the higher C_3A content, the lower the fluidizing effect. In the presence of alkali sulfate, the adsorption of superplasticizer on C_3A and C_4AF is inhibited, leading to increased adsorption on C_3S and C_2S . Consequently since the silicate phase adsorb a much lower amount of polymer than the aluminate phase does, an increase in the alkali content of the cement causes a reduction in the total amount of polymer adsorbed on cement, and this results in a higher amount of polymer in the aqueous phase to promote dispersion and reduction of the viscosity of the cement paste [17,18].

3.2. Characterization of the materials

Characterization can provide useful information about microstructural features of the cement slurries synthesized in this work. Figs. 3 and 4 show the Raman spectra of the standard slurry and epoxy-sp slurry, before and after HCl interaction. Using the Raman technique, spectra can be obtained for surface samples just a few microns thick and with minimal interference from the surrounding water [19]. In addition, spectra can be obtained rapidly, and extensive sample preparation is not needed.

The main information is related to silicate polymerization, presences of portlandite and TO_4 condensed tetrahedra in cement chains with T=Si or Al (Si-O-Si or Al-O-Si bonds) and possible identification of calcium carbonate polymorphs [19]. However, analysis of Raman spectra of cemented materials is difficult due to the presence of broad bands, band overlappings and fluorescence effects within cement minerals [20]. In addition, the presence of impurities in the crystalline structure of the silicate phases may cause modifications in the Raman spectra.

In the complex chemical composition of cement, alite and belite are the majority phases. For this reason and for the sake of simplification, cement composition is often likened to that of its silicate phases and more specifically to the majority alite phase. Alite is a C_3S -base solid solution and belite a C_2S -base solid solution. For all cemented samples, clear bands can be observed in the region $400\text{--}1800\text{ cm}^{-1}$. Only the strongest absorbing modes were assigned. The bands in the $800\text{--}900\text{ cm}^{-1}$ region are due to the Si-O group stretching vibrations in the C_3S and C_2S phases of the cement

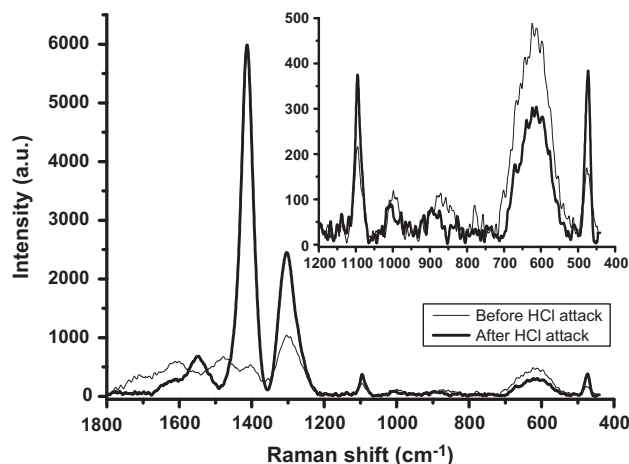


Fig. 3. Raman curves of the standard slurry before and after HCl attack.

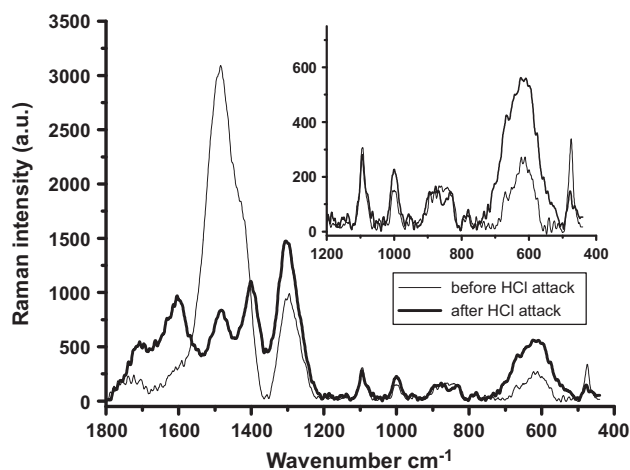


Fig. 4. Raman curves of the epoxy-sp slurry before and after HCl attack.

slurries [19]. The bands in the region from $450\text{ to }700\text{ cm}^{-1}$ are due to O-Si-O bending modes and to Si-O out-of-plane bending. The width of these bands is likely a reflection on the largely amorphous nature of the C-S-H gel. It can be noted the presence of a very small band at about 750 cm^{-1} region, suggesting the presence of very low amounts of aluminophases (C_3A) [21]. The band appearing at 1005 cm^{-1} is due to Si-O-Si symmetrical bending in the $-\text{C}_2\text{S}$ units. In addition, the SO_3 present in cement samples is probably to be found in the form of gypsum, a compound exhibiting a SO_4^{2-} vibration band at about 1010 cm^{-1} [22]. Consequently, this band may be due to the vibrations of both monosulfoaluminate and the silicate groups in the C_2S phase.

The wide band very likely encompasses the vibrations of the different forms in which calcium carbonate crystallizes (typically a mix of calcite, aragonite and vaterite), which generates a wide band that would combine the three chief vibration bands corresponding to carbonate groups in different environments, at about 1095 cm^{-1} [23]. Some authors suggest that the carbonate ion may replace the sulfate ion in the ettringite structure to form ettringite carbonate or thaumasite [24]. The carbonate and sulfate bands in thaumasite ($\text{Ca}_3\text{Si}(\text{OH})_6(\text{CO}_3)(\text{SO}_4) \cdot 12\text{H}_2\text{O}$) appear at about 1000 cm^{-1} and overlap with the carbonate and ettringite bands. The band at about 660 cm^{-1} , attributed to the vibrations of silicate groups in octahedral environments, would identify the presence of thaumasite, but as this band overlaps with the C-S-H gel band, the presence of this compound cannot be confirmed. The bands due to symmetrical C-O stretching vibrations of the carbonate group can be seen in the $1030\text{--}1500\text{ cm}^{-1}$ region. It can be an indication that carbonates are present in different chemical environments [25]. These carbonate groups are generated primarily by carbonation of the portlandite present in hydrated cements, which may take place at any of the various stages in the process, including hydration, drying, grinding and so on [25].

After HCl interaction, changes clearly take place in the region of $1200\text{--}1700\text{ cm}^{-1}$. The intensity of the band at 660 cm^{-1} , associated with C-S-H phase, declines substantially. On the other hand, the bands at about 475 and 1095 cm^{-1} increase in intensity, suggesting possible reorganization or recrystallization of the C-S-H and carbonates phases in the standard slurry. The intense band at 1410 cm^{-1} is an indication of the presence of CO_3^{2-} groups in calcite or crystallized calcium aluminosilicate hydrates [25].

The effect hinges on formation or dissolution of CO_3 -bearing minerals phases. During reaction with atmospheric pCO_2 , native calcite persists, whereas when CO_2 is excluded, CaCO_3 dissolution occurs [26]. Calcite dissolution affects aluminosilicate precipitation reactions directly because the Ca^{2+} released in the absence of CO_2

reacts with Al and Si from silicate mineral dissolution to form calcium aluminosilicate hydrates. In general, dissolution rates of minerals are most often controlled by their surface imperfections (dislocations). The kinks and steps at the crystal-edges can be termed as dislocation sites and are characterized by lower binding energies. The atoms of these sites are susceptible to detach themselves from the surface and are thus first to be released upon dissolution. However, the diffusion of Ca^{2+} and CO_3^{2-} ions away from the crystal surface of calcite is minimal because truly diffusion controlled dissolution is limited to highly soluble salt minerals and it results in general rounding of the mineral grains. In addition, the dense atomic packing of calcite can also decrease its dissolution rate in aqueous medium [26].

The identification of polymers within the cementitious matrix is a major problem, due to the low polymer amounts in the cement samples. Anyway, looking at the Raman spectra of the epoxy-sp slurry, it is supposed that the presence of the epoxy/superplasticizer polymeric net causes some reorganization of microstructure in relation to the standard slurry. The Raman spectrum shows a band at 830 cm^{-1} , suggesting the presence of a wide distribution of backbone polyacrylates, including helical structures and planar “zigzag” conformations over very short segments [27].

The presence of the polymeric net of epoxy/polyacrylate segments is proven by the presence of the absorption bands at 830 and 880 cm^{-1} associated with the C–H stretching vibration of the epoxide group and the C–O stretching of polyacrylate group [27]. However, these bands are broad and their intensities are low. It is noted the presence of several bands in the region of 1200 – 1800 cm^{-1} , which are assigned to carbonate groups with different local environments or due to the presence of acrylate species. There are no significant bands in the region below 950 cm^{-1} , allowing thaumasite and ettringite to be readily distinguished on the basis of the thaumasite octahedral Si peak at 650 cm^{-1} . An asymmetric broad band due to C=O stretching modes centers near 1500 cm^{-1} is observed [28]. The band at 1707 cm^{-1} has been assigned to C=O stretching modes of cyclic hydrogen-bonded COO^- groups in dimeric form of polyacrylates. In general, the C=O band widths of inner groups are much broader than those of other species, reflecting a broad distribution of the oligomer chains of variable lengths [28].

After HCl attack, two new bands appear in the C=O stretching region, which are located at 1710 and 1603 cm^{-1} . These bands may be assigned to an in-phase C=O stretching vibration of the cyclic dimer form of polyacrylate or to its C=O stretching modes of free COO^- groups, and terminal and inner COO^- in the oligomeric forms. The bands at 950 cm^{-1} would be due to compounds in which the sulfate groups bond to groups more voluminous than water. The band at 1010 cm^{-1} would be assigned to sulfate groups bonding to groups less voluminous than water, such as monosulfoaluminates [27,28].

The XRD profiles of the slurries are presented in Figs. 5 and 6. The potential uses of XRD powder diffraction in the study of clinker cement are related to the determination of phase composition, determination of polymorphic modifications and state of crystallinity of individual phases. However, the hydration products of cement do not have very clear diffraction peaks, due mainly to their semi-amorphous nature. XRD reflections from different minerals coincide or overlap. So, modifications of the composition of clinker hydration products can probably occur but they cannot be clearly evaluated by means of XRD. Difficulties in quantitative analysis are caused by variability of patterns of phases due to compositional or polymorphic variation, peak broadening due to compositional zoning and imperfect crystallinity. Moreover, the symmetry of the solid solutions changes, which affects X-ray intensities [29].

Calcium silicate hydrates possess a remarkable level of structural complexity. More than 30 crystalline calcium silicate hydrate

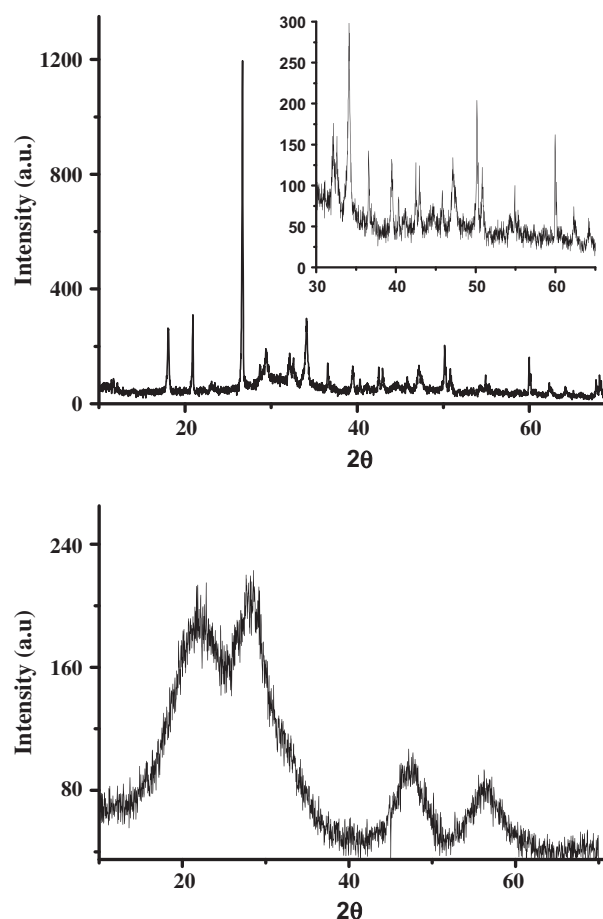


Fig. 5. DRX diffractogram of the standard slurry before (above) and after (below) HCl attack.

phases are known, and preparations made near room temperature have structures that range from semicrystalline to nearly amorphous, all of which are described by the generic term, “C–S–H”; more specific terms are used when necessary [30]. For the standard slurry, the main products are portlandite, ettringite and ill crystallized C–S–H with C/S ratio from 1.5 to 1.8 [31]. Crystal structure of ettringite has been subject of controversy due to its formation in hexagonal or trigonal crystallographic models. The main difference between these models is the number of crystallographic sites for the sulfate anions.

In general, ettringite has SO_4^{2-} groups with disorder occupation in hexagonal descriptions, or a relatively ordered trigonal description with three independent SO_4^{2-} tetrahedra. However, distinguishing these two models is rather difficult without ambiguity [32].

Alite is normally so much the predominant phase that its pattern tends to swamp those of the other phases. All the stronger peaks of belite are overlapped by ones of alite. It is suggested the formation of major products of portlandite [$\text{Ca}(\text{OH})_2$], ($2\theta = 18^\circ$), calcite and β -tricalcium silicate (C_3S , [$\text{Ca}_3\text{Si}_2\text{O}_7(\text{OH})_6$]), ($2\theta = 27^\circ$), ettringite, ($3\text{CaO} \cdot \text{Al}_2\text{O}_3 \cdot 3\text{CaSO}_4 \cdot 32\text{H}_2\text{O}$), ($2\theta = 34^\circ$) and a mixture of α -dicalcium silicate, (C_2S , [$\text{Ca}_2\text{SiO}_4 \cdot \text{H}_2\text{O}$]), portlandite, ($2\theta = 47^\circ$) [29], and tobermorite [$\text{Ca}_5\text{Si}_6\text{Al}(\text{OH})\text{O}_{17} \cdot 5\text{H}_2\text{O}$] (a strength retrogression inhibitor presents in cured oilwell slurries [1]), as well as mixtures of quartz, calcite and aragonite, ($2\theta = 21^\circ$ and 28°) [29]. For the epoxy-sp slurry, a relatively similar XRD profile was observed.

The presence of highly reactive silica in slurry composition enhances the polymerization of C–S–H, which precedes tobermorite formation, consequently inhibiting the rearrangement of C–S–H

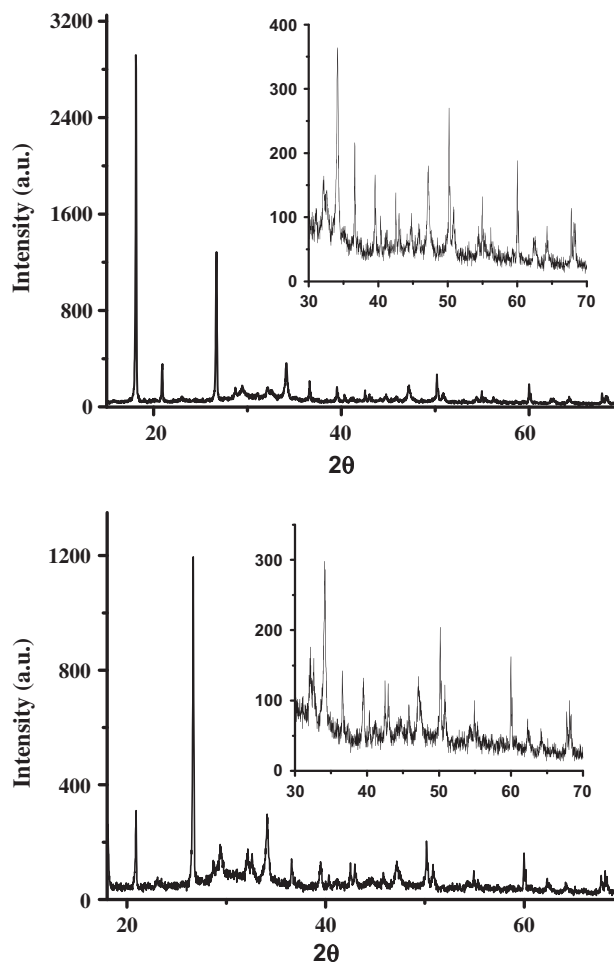


Fig. 6. DRX diffractogram of the epoxy-sp slurry before (above) and after (below) HCl attack.

to tobermorite [33]. On the other hand, the presence of Al slows the initial formation of C–S–H by reducing the solubility of quartz, which then accelerates tobermorite formation from C–S–H. Houston et al. reported that tobermorite formation proceeded via three steps: formation of amorphous and non-crystalline C–S–H, growth of semi-crystalline tobermorite, and recrystallization of solid tobermorite [33].

It has been reported that the C–S–H with high Ca/Si ratio tends to have short silicate chains and is more likely to be transformed into tobermorite than that with low Ca/Si [33]. In the C–S–H structure, Al atoms have coordination numbers of 4–6; but only a coordination number of 4 in tobermorite structure. In general, the Al atoms having coordination number of 4 are substituted preferentially into bridging tetrahedral sites at middle chain sites [34].

From observation of the XRD diffractograms of the standard slurry after HCl interaction, the crystalline features of this slurry decreased markedly. Thus, XRD does not allow the determination of the slurries constituents properly. On the other hand, the XRD diffractogram of the epoxy-sp slurry after HCl interaction is more or less the same in relation to this same material before HCl interaction. It seems to be an evidence that the epoxy-sp slurry remains its main crystalline features, even after HCl interaction.

The plots of TG/DTG are shown in Figs. 7 and 8. Thermal analysis (TG/DTG) can be used to determine quantitatively from the mass loss of the liquid (H_2O), gas (typically H_2O and CO_2), as well as to further analyze some cement phases that do not appear by the use of XRD technique which only shows the crystalline phases.

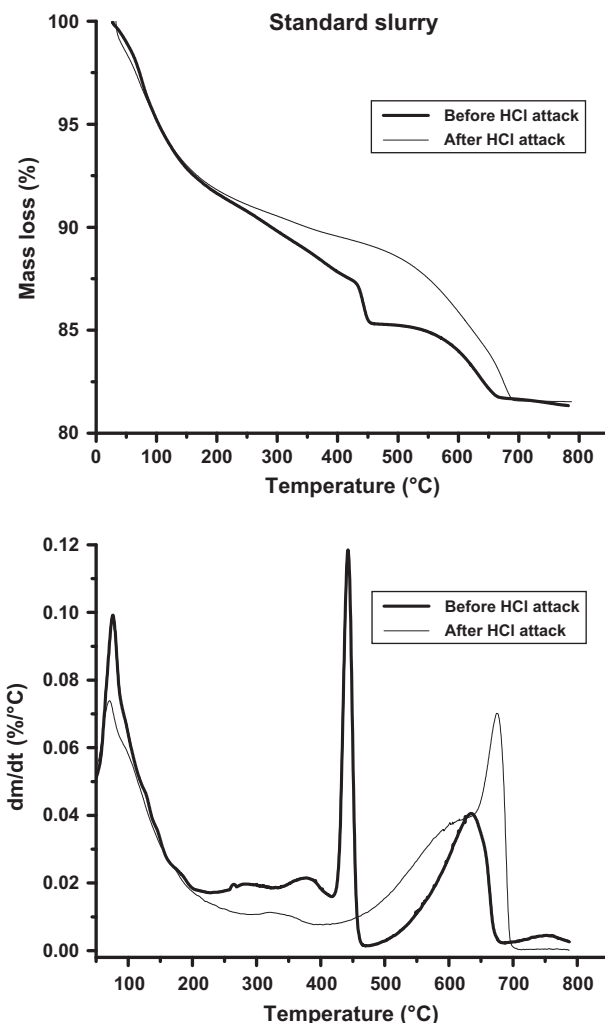


Fig. 7. TG (above) and DTG (below) curves of the standard slurry before and after HCl attack.

However, the identification of mineral components and their quantification using TG/DTG is not easy due to overlapping processes [35].

Upon heating, cement slurries have shown a continuous sequence of more or less irreversible decomposition reactions. The results obtained from TG for the standard slurry before HCl interaction have shown five main mass loss transitions: the release of evaporable adsorbed water (≈ 30 – $120^\circ C$), the decomposition of gypsum, with a double endothermic reaction, the decomposition of ettringite, the loss of water from part of the carboaluminate hydrates (≈ 120 – $190^\circ C$), the loss of bound water from the decomposition of the C–S–H and carboaluminate hydrates (≈ 190 – $420^\circ C$), the loss of water from portlandite dehydration (≈ 420 – $460^\circ C$), and the decomposition of the carbonate phases, typically calcium carbonate (≈ 475 – $700^\circ C$) [36].

A very small peak in the lap of the dehydration of C–S–H peak at about $170^\circ C$ is also observed. This reaction is very difficult to see in TG curves as it is just a slightly change of slope. This mass loss has been attributed to the decomposition of monocarboaluminates [35,36]. The dehydration reaction of the hydrates decreases gradually and can be considered as an irreversible reaction [37]. Ettringite decomposes to give monoaluminosulfates, which are themselves unstable at higher temperatures and are converted to a stable, crystalline hydrogarnet phase. After heating at $70^\circ C$, the short-range order is disrupted, and ettringite becomes amorphous

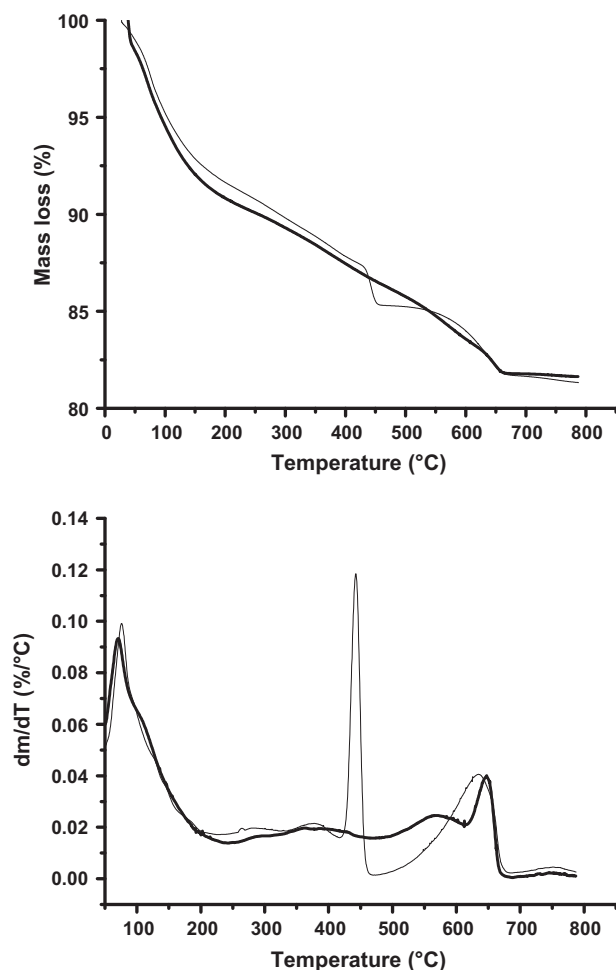


Fig. 8. TG (above) and DTG (below) curves of the epoxy-sp slurry before and after HCl attack.

in nature. Thereafter, the rest of the H_2O molecules in the columns and bridging OH groups in the Ca polyhedra are removed, and the frameworks of the columns are destroyed. This step is typically accompanied by changes in the coordination number of Al from 6 to 4 [37].

There are four well-characterized polymorphic forms of $-\text{C}_2\text{S}$ (γ , β , α' and α). Only the β and, occasionally, the γ forms are likely to occur in the cement clinker. Upon heating, γ - C_2S is converted to β - C_2S , from 480 to 950 °C [37].

From TG/DTG curves, the portlandite content was determined using the following Eq. (2) [38]:

$$\text{CH} (\%) = \frac{\Delta_{\text{CH}} (\%) \times M_{\text{CH}}}{M_{\text{w}}} \quad (2)$$

where CH (%) is the content of portlandite, $\Delta_{\text{CH}} (\%)$ is the weight loss during the dehydroxylation of calcium hydroxide, M_{CH} is the molar weight of calcium hydroxide and M_{w} is the molar mass of water.

For the standard slurry and the epoxy-sp slurry, the content of portlandite was found to be 8.23%. After HCl interaction, for both slurries, it can be clearly observed that the weight loss related to the dehydroxylation of portlandite is undetectable. It has been shown that the presence of organic polymers can significantly influence the morphology of portlandite in cement matrices, depending on the type and the brand of polymer, the polymer-to-cement ratio or a combination of all these factors. Because portlandite crystals represent the weak phase in the binder matrix and the surfaces of those crystals form preferred cleavage sites, the

strengthening by polymer bridges improves the overall strength of the binder matrix [39]. It is assumed that polymer particles act as a kind of a bonding agent between the different layers, increasing the interparticle bonding, but the presence of the polymers between the crystal layers could not be detected.

In this work, solid-state diffuse reflectance (DR) absorption spectroscopy is used to complement the morphological studies, because this technique is sensitive to changes in chemical environments of solid samples. However, the attribution of DR peaks is open to speculation. Band overlapping and poor spectral resolutions have generally precluded details of the chemical environment of Fe oxides in cement systems by DR [40,41]. The DR spectra of the slurries are shown in Fig. 9.

The DR spectrum of the standard slurry shows a broad absorption band at the visible wavelengths with a maximum absorption at about 580 nm. After HCl interaction, the maximum absorption of this broad band is shifted to about 620 nm. These two absorption bands have been considered to be associated with crystal field absorptions of Fe(III) in octahedral coordination with oxygen in hematite (580 nm) and ferrihydrite (620 nm) [41]. Analysis of the DR spectra has indicated relatively small changes in the DR spectra of the epoxy-sp slurry after HCl interaction. This suggests that the acidic interaction was little to affect the geometry of the central metal ions of the Fe(III) oxides in the modified cement slurry.

Cured cement slurries typically contain 3–6% of oxide impurities, chiefly Al_2O_3 and Fe_2O_3 . Trace metals associate with Fe(III) oxides as adsorbed or coprecipitated species can be found in cemented

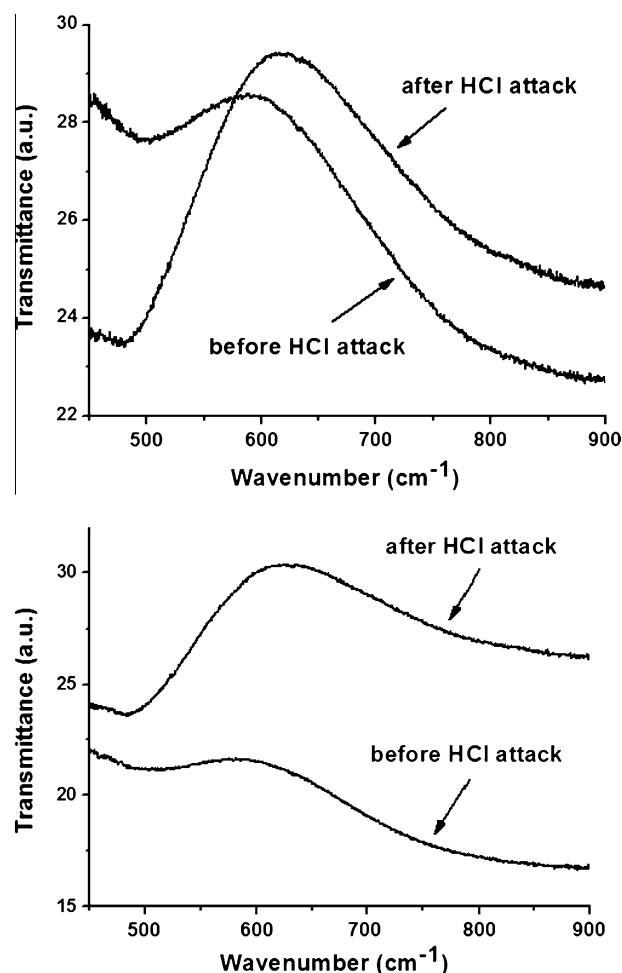


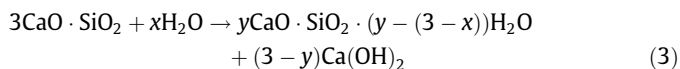
Fig. 9. Diffuse reflectance spectra of the standard slurry (above) and the epoxy-sp slurry (below), before and after HCl attack.

bodies. Fe(III) oxides with discrete amorphous or crystalline phases are high in surface area, form particle coatings of complex and varied composition, and are reactive [40,41]. Valence II and III metal cations can isomorphously substitute in the crystalline Fe(III) oxide structure (e.g., goethite and hematite). In alkaline conditions, Fe(III) oxides possess a goethite/akaganeite-like local structure around Fe. However, we are unable to give additional details of the transformation of hematite to ferrihydrite in the presence of HCl, using the experimental results of this work. In addition, detailed reactional aspects of iron oxides are assumed to be beyond the scope of this work.

Characterization has pointed out similarities between the cement slurry with the presence of the new epoxy/superplasticizer polymeric net, before and after HCl interaction. It underlines the good stability of this new type of cement slurry in the presence of high concentrations of acidic species in aqueous solution.

3.3. Energetic hydration features of the slurries evaluated by microcalorimetry

As cement hydrates, a significant amount of energy is released as heat. This heat of hydration must be included in any early-age model of heat transfer in cemented bodies. The heat released is dependent on the phase composition of the cement and the mass-normalized heat release can be either increased or decreased depending on the mineral admixture employed. At ambient conditions, tricalcium silicate reacts with water in an exothermic reaction to form calcium silicate hydrate with lower calcium content than the starting material and portlandite (CH) as a side product. The cement hydration can be expressed in the following general equation [42]:



The calorimetric results of the hydration process are shown in Table 1. Records were taken for the first 48 h of hydration, when the base lines of the calorimetric curves became unchanged.

In initial minutes after adding water, quick release of heat takes place, related to the effect of binder grains wetting, their partial dissolving of the surface, and the initial stage of ettringite formation. Soon after the first wetting, an initial rapid exothermic reaction (stage 1) appears due to a surface hydrolysis and the release of ions into solution. The first stage is high in heat releasing, due also to initial hydrolysis of the aluminous phase and the sulfoaluminous phase of the slurries [43]. However, the heat releases of these reactions overlap one another. Although the hydration reactions continue after this final peak, the rate declines substantially. In this work, the heat releases were observed to remain almost constant after about 40 h of hydration time.

Deceleration of the heat evolution is typically caused by the formation of metastable C—S—H on the surface of C₃S and retarded dissolution. The induction period (stage 2) is characterized by an increasing Ca(OH)₂ supersaturation and retarded nucleation of final products. The time at which the maximum supersaturation is reached before Ca(OH)₂ begins to crystallize at a significant rate, strongly depends on the reactivity of C₃S and the water-to-solid ratio [43]. During the second deceleration period (stage 3), the

growth of hydration products continues into empty spaces and is followed by the final slow reaction (stage 4) with a gradual densification of the microstructure, recrystallization of Ca(OH)₂ associated with a continued hardening [14,15].

The hydration enthalpy ($\Delta_{\text{int}}H$) of the cement slurries can be calculated directly by the following Eq. (4) [8,9]:

$$\Delta_{\text{int}}H = \frac{Q_{\text{int}}}{n_{\text{int}}} \quad (4)$$

where Q_{int} the integral interaction energy (J g⁻¹) and n_{int} is the number of moles of water sorbed per gram of the cemented specimen in the calorimeter cell (mol g⁻¹).

The total heat generated was calculated as the integral delimited by the heat release rate versus hydration time. It should also be known that the heat measured from solution microcalorimetry is an integral heat since there are different compounds produced in hydration of cement slurries. The standard slurry and the epoxy-sp slurry present similar results in terms of the integral energies released in the hydration processes.

The enthalpies of the hydration processes of the slurries are slightly exothermic in nature. Exothermic heats of reaction indicate the dominance of attractive forces in cement gel. The magnitude of hydration energies become less exothermic as the hydration time is increased. This decrease in the released hydration energies has been attributed to repulsive lateral interactions between hydrated species in cement gel; these repulsive interactions increased in magnitude as the interaction increased [44,45]. At higher loading, repulsive lateral interactions between the hydrated species, which are endothermic, might increase, decreasing the exothermic net heat of interaction at higher loadings.

In general, low exothermic interactions at solid and liquid interfaces are also in agreement with diffusion of fluidic phase (water) into internal interaction sites of the solid phase. It has been suggested that the small magnitude of the hydration enthalpies is an average result of diffusional (endothermic) and chemical bonding (exothermic) processes. Interactions at solid and liquid interfaces that occur with intense adsorbate diffusion present low values of $\Delta_{\text{int}}H$. Water transport through porous materials is generally described following an adsorption–diffusion mechanism, where molecules first diffuse from the bulk phase to the adsorbent surface. Next, they adsorb to the sites on the surface and diffuse through the adsorbent structure, driven by the chemical potential gradient within the pores.

3.3.1. Kinetic modeling of the hydration processes of the slurries from microcalorimetry

Kinetic data are the foundation of mechanistic investigations, and many of the systems of interest at solid and liquid interfaces are complex and present considerable difficulties in analysis. In this work, the kinetic modeling was performed using isotherms from the cumulative heat of hydration curves. In order to obtain accurate kinetic parameters, it is necessary to correct the values of the microcalorimetric outputs by applying Tian equation (Eq. (5)) [45]:

$$S_{\text{corr}}(t) = S_{\text{orig}}(t) + \tau \left(\frac{dS_{\text{orig}}(t)}{dt} \right) \quad (5)$$

where $S_{\text{corr}}(t)$ is the corrected calorimetric signal (W), $S_{\text{orig}}(t)$ is the original calorimetric signal (W), τ is the time constant of the calorimeter (150 s, in this work), and $[dS_{\text{orig}}(t)/dt]$ is the time derivative of the original calorimetric signal.

The Tian-corrected calorimetric outputs were fitted to a simple three-parameter kinetic function, as shown in Eq. (6) [8,9,44]:

$$Q_r = Q_r^m (1 - \exp^{-[k \cdot t]^n}) \quad (6)$$

Table 1
Calorimetric results of the hydration processes of the cement slurries.

Slurry	n_{int} (μmol/g)	$-Q_{\text{int}}$ (J/g)	$-\Delta_{\text{int}}H$ (kJ/mol)
Standard	25.4	0.697	27.44
Epoxy-sp	16.6	0.988	59.52

Average SD of the results: 4.7%.

where k is the kinetic constant and n is another constant, which is related to the kinetic order and the hydration mechanism of the slurries. The parameters Q_r and Q_r^m denote the energy released at given time t and the maximum energy released of the hydration processes, respectively.

A nonlinear methodology was used for calculating and analyzing the kinetic parameters [8,9]. The results are shown in Table 2. The comparative plots of the experimental and calculated hydration energies (Q_r) in relation to the three-parameter kinetic model are shown in Fig. 10.

In order to analyze the fitting of the kinetic model, chi-square tests were carried out according to the following equation:

$$\chi^2 = \sum \frac{(Q_{r,e} - Q_{r,m})^2}{Q_{r,m}} \quad (7)$$

where $Q_{r,e}$ and $Q_{r,m}$ are the calorimetric outputs, which were calculated using experimental data and an specific kinetic model, respectively.

The chi-square statistic test is basically the sum of the squares of the differences between the experimental data and theoretically predicted data from models. If modeled data are similar to the experimental data, χ^2 will be a small number; if they are different, χ^2 will be a large number [8,9]. From inspection of Table 2, good agreements of the experimental and calculated data were found for the hydration processes of both cement slurries. However, the fit of some values at the end of the hydration processes was relatively poor (details not shown). This seems to suggest that the cement hydration reactions did not stop at the stage of the end of the last plateau, after about 48 min of hydration time.

The introduction of organic polymeric additives into cement paste makes the hydration rate get reduced, and the value of the kinetic constant k of heat release of the epoxy-sp slurry is lower in comparison with the standard slurry one. By analyzing the different hydration theories, several explanations can be found for the retardation of the cement hydration reactions in the presence of organic polymers, such as adsorption, nucleation control and poisoning of the crystal growth, complexation of the rate-controlling alkalis, precipitation of insoluble complexes hindering the water transport, incorporation in the protective membrane around the cement particles and decreased ion mobility. Probably, not just one mechanism is sufficient to explain all aspects of retardation, but rather a combination of interactions [46]. The complexation of metal ions (typically Fe(III)) in the water-soluble polymers can occur. By complexing these ions, the solubility of the ions may increase, the early precipitation of hydration products is prevented and more cement compounds should be dissolved before hydration barriers are set up. Besides the adsorption on the unhydrated particles, adsorption on the hydrating compounds can also occur. The adsorption of polymers on the $\text{Ca}(\text{OH})_2$ and C–S–H nucleation sites can “poison” the growth of those phases.

Water-soluble polymers increase the viscosity of the mixing water, which restricts the movement of ions and decreases the dissolution rate of the unhydrated phases and the precipitation of hydrates. Typically, water-soluble polymers extend the induction period and interfere with early cement hydration reactions. This effect is caused mainly by the replacement of part of the cement with a less reactive material (the epoxy/superplasticizer polymeric

Table 2

Kinetic parameters of the hydration of the slurries from the exponential three-parameter kinetic model.

Slurry	Q_r^m (mW)	$k/10^{-3}$ (h^{-1})	n	χ^2
Standard	1453	56.0	0.621	51.7
Epoxy-sp	1506	0.0007	0.650	21.5

Average SD of the results: 5.8%.

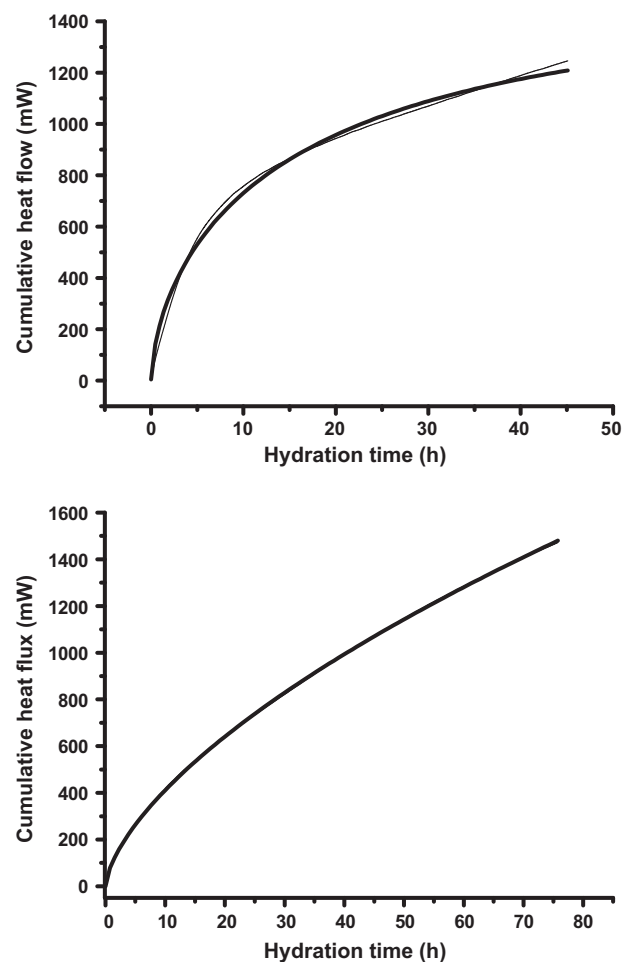


Fig. 10. Plots of experimental (thin lines) versus predicted (thick lines) values for the nonlinear analysis of the three-parameter kinetic model of the hydration processes of the cement slurries.

phase). Polymers can also be adsorbed on the unhydrated cement particles, preventing the reaction by water [46].

The mechanistic interpretation of the kinetic constant n is difficult and open to discussion. In general, the values of n from 0.9 to about 1.2 have been related to surface reactions and from 3 to about 4 to three-dimensional interactions at solid and solution interfaces. When interaction occurs on specific sites, interactions may be random leading to high values for n (2, 3 or higher). In last stages of equilibrium, the interaction may be restricted to one or two dimensions. So, saturation may lead to n values of 1, 2 or 3 for surface, edge and point sites in internal sites of the adsorbent, respectively. In this work, the values of this kinetic parameter ($n \sim 0.6$) suggest that the hydration of the cement slurries is mainly governed by diffusion growth into non-stoichiometric mixtures in cement gel [47]. It is worth to be noted that both the kinetic and thermodynamic results are in agreement with diffusion growth as the main mechanistic feature of the cement slurries hydration.

In order to obtain more details of the features of the slurries evaluated in this work, further research, such as using solid-state NMR spectroscopy, should also be used.

4. Summary

In this study, a new epoxy/superplasticizer-modified cement slurry was synthesized. Characterization has pointed out similarities between the cement slurry with the presence of the epoxy/

superplasticizer polymeric net, before and after HCl interaction. Solution microcalorimetry was used to assess the energetic parameters of hydration of the slurries. The values of Q_{int} and $\Delta_{int}H$ are all low exothermic in nature. The standard slurry and the epoxy-sp slurry present similar results in terms of the integral energies released in the hydration processes. The kinetic data of the microcalorimetric outputs of the hydration processes were well fitted to a three-parameter model. The analysis of the kinetic and thermodynamic results is in good agreement with diffusion growth as the main mechanistic feature of the cement slurries hydration.

The results of this study underline the excellent features of the new epoxy/superplasticizer-modified cement slurry for using in routine oilwell operations.

References

- [1] P.C. Hewlett (Ed.), *Lea's Chemistry of Cement and Concrete*, Elsevier, Burlington, 1998.
- [2] B. Huet, V. Tasoti, I. Khalfallah, *Energ. Procedia* 4 (2011) 5275.
- [3] S. Portier, F.-D. Vuataz, P. Nami, B. Sanjuan, A. Gerard, *Geothermics* 38 (2009) 349–359.
- [4] H.W. Dörner, R.E. Beddoe, Prognosis of concrete corrosion due to acid attack, in: 9th International Conference of Building Materials, Brisbane, Australia, 2002.
- [5] D.A. Silva, P.J.M. Monteiro, *Cem. Concr. Res.* 35 (2005) 351.
- [6] F. Djouani, C. Connan, M.M. Chehimi, K. Benzarti, *Surf. Interface Anal.* 40 (2008) 146.
- [7] E.M. Petrie, *Epoxy Adhesives Formulations*, Mc-Graw-Hill, New York, 2006.
- [8] A.R. Cestari, E.F.S. Vieira, F.C. da Rocha, *Thermochim. Acta* 430 (2005) 211.
- [9] A.R. Cestari, E.F.S. Vieira, A.M.G. Tavares, M.A.S. Andrade Jr., *J. Colloid Interface Sci.* 343 (2010) 162.
- [10] K. Yamada, *Cem. Concr. Res.* 41 (2011) 793.
- [11] W. Nocun-Wcelik, Z. Konik, A. Stok, *Constr. Build. Mater.* 25 (2011) 939.
- [12] R.E. Beddoe, H.W. Dörner, *Cem. Concr. Res.* 35 (2005) 2333.
- [13] V. Ershadi, T. Ebadi, A.R. Rabani, L. Ershadi, H. Soltanian, *Int. J. Environ. Sci. Dev.* 2 (2011) 128.
- [14] J.F. Young, *Cem. Concr. Res.* 1 (1971) 113.
- [15] A. Popova, G. Geoffroy, *J. Am. Ceram. Soc.* 83 (2000) 2556.
- [16] R. Mezzenga, L. Boogh, J.-A.E. Månson, *Compos. Sci. Technol.* 61 (2001) 787.
- [17] M. Kismi, J.-C. Saint-Arroman, P. Mounanga, *Constr. Build. Mater.* 28 (2012) 747.
- [18] A. Papo, L. Piani, *Cem. Concr. Res.* 34 (2004) 2097.
- [19] S. Martinez-Ramirez, M.F. Concepción, *J. Raman Spectrosc.* 37 (2006) 555.
- [20] S.P. Newman, S.J. Clifford, P.V. Coveney, V. Gupta, J.D. Blanchard, F. Serafin, D. Ben-Amotz, S. Diamond, *Cem. Concr. Res.* 35 (2005) 1620.
- [21] L. Black, C. Breen, J. Yarwood, C.-S. Deng, J. Phipps, G. Maitland, *J. Mater. Chem.* 16 (2006) 1263.
- [22] S.N. Ghosh (Ed.), *Advances in Cement Technology: Chemistry, Manufacture and Testing*, Tech Books International, New Delhi, 1983.
- [23] M.Y.A. Mollah, W. Yu, R. Schennach, D.L. Cocke, *Cem. Concr. Res.* 30 (2000) 267.
- [24] S. Kohler, D. Heinz, L. Urbonas, *Cem. Concr. Res.* 36 (2006) 697.
- [25] P. De Silva, L. Bucea, V. Sirivivatnanon, *Cem. Concr. Res.* 39 (2009) 460.
- [26] S.K. Yadav, G.J. Chakrapani, M.K. Gupta, *Environ. Geol.* 53 (2008) 1683.
- [27] J. Dong, Y. Ozaki, K. Nakashima, *Macromolecules* 30 (1997) 1111.
- [28] M. Todica, E. Dinte, C.V. Pop, C. Farcau, S. Astilean, *J. Optoelectr. Adv. Mater.* 10 (2008) 823.
- [29] F. Djouani, C. Connan, M. Delamar, M.M. Chehimi, K. Benzarti, *Constr. Build. Mater.* 25 (2011) 411.
- [30] G. Le Saout, É. Lécolier, A. Rivereau, H. Zanni, *C. R. Chimie* 7 (2004) 383.
- [31] C. Shi, J.A. Stegemann, *Cem. Concr. Res.* 30 (2000) 803.
- [32] M. Chrysochoou, D. Dermatas, *J. Hazard. Mater.* 136 (2006) 20.
- [33] J.H. Houston, R.S. Maxwell, S.A. Carroll, *Geochem. Trans.* 10 (2009) 1.
- [34] K. Matsui, J. Kikuma, M. Tsunashima, T. Ishikawa, S. Matsuno, A. Ogawa, M. Sato, *Cem. Concr. Res.* 41 (2011) 510.
- [35] A. Chaipanich, T. Nochaiya, *J. Therm. Anal. Calorim.* 99 (2010) 487.
- [36] L. Alarcon-Ruiza, G. Platret, E. Massieu, A. Ehrlicher, *Cem. Concr. Res.* 35 (2005) 609.
- [37] S.M. Antao, M.J. Duane, I. Hassan, *Can. Mineral.* 40 (2002) 1403.
- [38] E.F.S. Vieira, A.R. Cestari, R.G. da Silva, A.A. Pinto, C.R. Miranda, A.C.F. Conceição, *Thermochim. Acta* 419 (2004) 45.
- [39] A. Jennia, L. Holzerb, R. Zurrigenc, M. Herwegh, *Cem. Concr. Res.* 35 (2005) 35.
- [40] T. Nagano, S. Nakashima, S. Nakayama, K. Osada, M. Senoo, *Clays Clay Miner.* 40 (1992) 600.
- [41] J. Torrent, V. Barrón, Diffuse reflectance spectroscopy of iron oxides, in: *Encyclopedia of Surface and Colloid Science*, Marcel Dekker, New York, 2002.
- [42] D.C. MacLaren, M.A. White, *J. Chem. Educ.* 80 (2003) 623.
- [43] D.P. Bentz, *Cem. Concr. Res.* 38 (2008) 196–204.
- [44] I. Wadso, *Chem. Soc. Rev.* 26 (1997) 79.
- [45] W. Plazinski, W. Rudzinski, A. Plazinska, *Adv. Colloid Interface Sci.* 152 (2009) 2.
- [46] Ki-Bong Park, T. Noguchi, J. Plawsky, *Cem. Concr. Res.* 35 (2005) 1676.
- [47] R.S. Disselkamp, S.E. Anthony, A.J. Prenni, T.B. Onasch, M.A. Tolbert, *J. Phys. Chem.* 100 (1996) 9127.